Full Length Article

Mathematical model for predicting the performance of photovoltaic system with delayed solar irradiance

Siti Nurashiken Md Sabudin [a], Norazaliza Mohd Jamil [b,*]

[a] Department of Science & Mathematics, IPG Kampus Tengku Ampuan Afzan, 27200, Kuala Lipis, Pahang, Malaysia
[b] Centre for Mathematical Sciences, Universiti Malaysia Pahang Al-Sultan Abdullah, Lebuhraya Persiaran Tun Khalil Yaakob, 26300, Gambang, Kuantan, Pahang, Malaysia

ARTICLE INFO

ABSTRACT

Photovoltaic systems convert solar irradiance into electricity. Due to some factors, the amount of solar irradiance arriving at the solar photovoltaic collector at a specific location varies. The goal of this study was to develop a mathematical model for predicting the performance of a photovoltaic system, which depends on the amount of solar irradiance. A novel model for solar irradiance in the form of a delay differential equation is introduced by including the factor of delayed solar irradiance, hour angle and the sun's motion. The simulation study is carried out for the three scenarios of weather conditions: a clear day, a slightly cloudy day, and a heavily overcast day. The numerical solution is obtained by adopting the 4th-order Runge Kutta method coupled with a parameter fitting technique, the Nelder Mead algorithm, which is implemented by using MATLAB software. The data from a solar plant in Pahang, Malaysia, was used for model validation and it is found that the prediction profile for solar irradiance aligns well with the intermediate and decay phases, but deviates slightly during the growth phase. The output current and power for the solar photovoltaic panel were treated as time-dependent functions. As the solar irradiance increases, the output current and power of the solar panel will increase. The result showed that the maximum output current and output power of STP250S-20/Wd crystalline solar module decreased by 42% and 76%, respectively, during slightly cloudy and heavily overcast conditions when compared to clear days. In other words, the performance of a photovoltaic module is better on clear days compared to cloudy days and heavily overcast. These findings highlight the relationship between delayed solar irradiance and the performance of the solar photovoltaic system.

1. Introduction

Renewable energy could diversify energy resources in electricity generation and reduce dependency on depleting fossil fuels (Jamil and Wang, 2016). Compared to fossil fuels, solar technology is the fastest-growing, most cost-effective, and least harmful to the environment. Solar irradiance is an essential source of energy conversion for solar photovoltaic (PV) systems. According to Widén & Munkhammar (2019), the amount of solar irradiance arriving on the PV panel consists of three components, i.e., direct, diffuse, and reflected, influenced by weather conditions.

The overwhelming response to solar PV systems as a new electricity resource provided research opportunities to improve the system and meet the current needs. Mathematical modelling took part as a solution for presenting the actual situation. The existing models were designed based on the specific hardware, factor, environment, and manufacturer information, making them non-uniform. Consequently, adapting existing formulas to the chosen hardware model remains a challenge.

The amount of solar irradiance arriving on the PV panel is the primary factor influencing the output current. Various models, such as artificial neural networks (ANNs) (Al-Fatlawi et al., 2015; Khatib et al., 2012), global horizontal irradiance (Chow et al., 2011), geographical information system (Rumbayan et al., 2012) and linear model (Rosario, 2014; Danandeh, 2018) had been employed to estimate solar irradiance. Factors influencing the solar irradiance amount on the flat panel include geometrical parameters, sunshine parameters, simulation days and temperature (Arief et al., 2017; Khatib et al., 2012; Mekhilef et al., 2012; Moballegh and Jiang, 2014; Rizal and Wibowo, 2013; Rosario, 2014; Shukla et al., 2015; Zaatri and Azzizi, 2016; Jiang, 2008; Hasni et al., 2012; Ozgoren et al., 2012; Chen et al., 2013). However, none have

---

* Corresponding author.
E-mail address: norazaliza@umpsa.edu.my (N. Mohd Jamil).

adequately demonstrated a sufficiently meaningful parameter related to delay time.

The output current and power values contribute to the measurement of the performance of a solar PV system. However, the existing mathematical model for solar PV panels formulated the output current and power as a static value (constant and time-independent). In reality, the value of a solar PV panel's output current and power varies and keeps changing over time due to the fluctuating amount of solar irradiance arriving on the solar panel. This results in inaccurate performance estimation under the oscillating amount of solar irradiance. A clear linkage between the solar irradiance model and the output current and power of solar PV is essential to obtain a better understanding of the performance of the PV system. For this purpose, research is needed to integrate solar irradiance into the performance of solar PV in a seamless fashion.

Therefore, this study aimed to present a new model for predicting the solar irradiance arriving on the PV panel by using a delay differential equation (DDE). To the best of our knowledge, no deterministic model in

model in the form of DDE to simulate the dynamics of climate change with limited parameters. Their study proved that delays have a significant impact on the behavior of the real situation. Moreover, Keane et al. (2017) utilized DDE to model a system that demonstrated chaotic behavior representing the irregularity characteristic of El Niño–Southern Oscillation (ENSO).

In this study, the dynamics of solar irradiance arriving on the PV panel are viewed as a compartmental model, as illustrated in Fig. 1. This compartmental model framework is used as a backbone to formulate a model. This process has inputs and outputs from the 'compartment' over time. In this case, the compartment is the rate of solar irradiance, $G(t)$. The inputs are direct solar irradiance and diffused solar irradiance. Meanwhile, the output occurs through reflected solar irradiance. We are interested in the amount of solar irradiance arriving on the PV panel at any given time.

Based on the compartmental model in Fig. 1, the rate of change of solar irradiance arriving on a PV panel is equal to the 'rate in' minus the 'rate out', and the balance law can be written as follows:

$$\left\{ \begin{array}{c} \textit{Rate of change of solar irradiance} \\ \textit{on the solar photovoltaic panel} \end{array} \right\} = \left\{ \begin{array}{c} \textit{Rate of incoming solar irradiance i.e.} \\ \textit{sum of direct and diffuse solar irradiance} \end{array} \right\} - \left\{ \begin{array}{c} \textit{Rate of outgoing solar irradiance} \\ \textit{i.e. reflect solar irradiance} \end{array} \right\}$$

the form of an ordinary differential equation (ODE) has been proposed to describe the dynamic of solar irradiance. Furthermore, the dependence of solar irradiance on delay time has yet to be discovered. Hence, this study will adopt this approach in formulating the time-dependent solar irradiance. Subsequently, the resulting solution of solar irradiance will be used to predict the performance of the PV system by means of calculating the solar PV's output current and power.

2. Mathematical modelling

Mathematical modeling translates the real-world process into estimation calculation that can be used to study the behavior of a process. Many authors have developed a model for solar irradiance, mostly applying stochastic models, time series models, and neural networks. Evolution in differential equations has grown and has been applied in many fields. However, no research formulated a deterministic model such as an ODE for solar irradiance, and less research used a delay factor in their model. In this study, a new mathematical formulation for solar irradiance in the form of a DDE was developed. DDE is a differential equation in which the derivatives of a function at the present time rely on the values of the functions at earlier times, called delay. Note that the DDE model is a complicated ODE model considering that phenomena may have a delayed effect (Shampine and Thompson, 2009).

DDE has been used for various physical systems in previous research, such as ecology (Kolesov and Shvitra, 1979), control theory (Pyragas, 2006), genetics regulatory systems (Parmar et al., 2015; De Jong et al., 2021), neural systems (Campbell, 2007; Schöll et al., 2009; Rahman et al., 2018), epidemics (Kyrychko and Blyuss, 2005), coupled chemical oscillators (Blaha et al., 2013) and laser system (Lenstra and Yousefi, 2000; Krauskopf, 2005). Keane et al. (2017) introduced a mathematical

In the next step, this balance-law approach is used to formulate mathematical models of differential equations that describe the dynamics of solar irradiance on the solar PV panel. Let $G(t)$ be the amount of solar irradiance on the PV module at a given time t (in minutes). The newly proposed delay differential model for solar irradiance is given in Equation (1).

$$\frac{dG(t)}{dt} = \alpha - \beta G(t)\dot{R}(t - \tau) \tag{1}$$

The parameter α is the constant rate of the direct and diffused solar irradiance arriving on the solar panel and β is a constant. $\dot{R}(t)$ is the decay rate of solar irradiance outgoing from the solar panel due to reflected solar irradiance, hour angle and the sun's motion and is assumed to follow the Hill function, that is $\dot{R}(t) = \frac{(G(t))^n}{\theta^n + (G(t))^n}$. Hill function is a monotonic increasing function of $G(t)$ that meets the following features: If $G(t) = 0$, then $\dot{R}(t) = 0$, if $G(t) = \theta$, then $\dot{R}(t) = 1/2$, and $\lim\limits_{G(t) \to \infty} \dot{R}(t) = 1$.

The detection of solar irradiance at the solar panel is not an instantaneous process; there is a time lag because the solar irradiance transportation from the sun to the solar panel requires time. The time delay, τ is the time taken by the solar irradiance reached on the solar PV panel after initiation that relates to diffused and reflected solar irradiance. On top of this, there is a significant delay between the elimination of solar irradiance and the measurement of solar irradiance collected on solar PV.

Thus, the rate of change of solar irradiance on the solar panel can be rewritten as in Equation (2),

$$\frac{dG(t)}{dt} = \alpha - \frac{\beta G(t)(G(t - \tau))^n}{\theta^n + (G(t - \tau))^n} \tag{2}$$

where α, β, θ, and n are positive constant and $\tau > 0$. The parameter α is related to the production rate while, β, θ, and n determines the decay rate of solar irradiance. The initial function is stated in Equation (3).

$$G(t) = \varphi(t) \text{ for } -\tau \le t \le 0, \text{ where } \varphi \in C[[-\tau, 0], \mathbb{R}^+] \text{ and } \varphi(0) > 0 \tag{3}$$
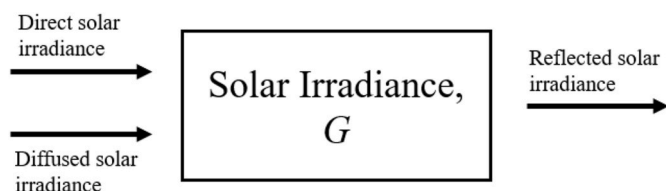

Fig. 1. Compartmental model.

In developing the proposed model, the following assumptions are adopted.

i. The rate of direct solar irradiance striking the atmosphere/earth and the diffused solar irradiance, α, is constant. It is independent of a solar panel's collected amount of solar irradiance.
ii. We assume that the collected solar irradiance on the solar panel can only change due to the amount of direct, diffused, and reflected solar irradiance.
iii. The model involves two mechanisms. The positive mechanism is through the direct and diffused solar irradiance that arrives on the solar collector. The negative one is due to the reflected solar irradiance in which the solar irradiance turns back to the atmosphere, hour angle, and the sun's motion.
iv. We assume that the weather conditions, such as cloudiness, sky clearness index, humidity, and wind, are consistently similar for each day within specific model's simulation.
v. Subsequently, we assume that the removal of solar irradiance on the solar panel at any time is proportional to the amount of the collected solar irradiance at a previous time $\tau > 0$. Time delay plays a vital role in simulating the amount of solar irradiance reflected by the surface of the PV module.

The forecasting model of solar irradiance can give a rough approximation of the performance of solar PV. The above-proposed approach to predicting solar irradiance can be subsequently applied to predicting solar power performance. Note that the PV system's instantaneous output power will change with time as the amount of solar irradiance collected by PV cells varies from morning to night, day to day, weeks to weeks, and months to months.

This study focuses on the PV circuit model with a single diode model with five parameters (Sabudin et al., 2017, 2020; Sabudin and Jamil, 2019). The equation for the output current, I_0 (in Ampere, A) is given by (Phang et al., 1984):

$$I_0 = I_{PV} - I_D - I_{SH}$$

where

$$I_D = I_{RC}\left[\exp\left(\frac{V + IR_S}{aV_T}\right) - 1\right]$$

$$I_{SH} = \frac{V + IR_S}{R_{SH}}$$

$$V_T = \frac{kT}{q}N_S$$

The parameter I_{PV} is the photocurrent, I_0 is the current, which flows through the parallel diode, and I_{SH} is the shunt current flown due to the presence of R_{SH}, (Phang et al., 1984). The symbol q is the electron charge ($1.60217646 \times 10^{-19}$ C), k is the Boltzmann constant $1.3806503 \times 10^{-23}$ J/K, V_T is the thermal voltage for a cell, which is influenced by temperature T, N_S is the number of cells, I_{RC} is the current flow inside the diode that influences the amount of I_D, and a is the ideality diode. The output power, P_0 is given by;

$$P_0 = I_0 V$$

Table 1
Dimensions of parameters.

Parameters	Value
$G(t), \theta$	W/m^2
α	W/(m^2 min)
β	1/min

3. Linear stability analysis

Dimensions of parameter quantities in the newly proposed solar irradiance model are given in Table 1.

We introduce dimensionless variables and parameters into the model as

$$y = G/\theta, s = \beta t, \sigma = \beta \tau \text{ and } c = \alpha/\theta\beta \quad (4)$$

After substituting the variables and simplifying the equation, we obtained

$$\frac{dy}{ds} = \frac{\alpha}{\theta\beta} - \frac{\beta}{\theta\beta}y\theta\frac{\theta^n(y(s-\sigma))^n}{\theta^n[1+(y(s-\sigma))^n]} \quad (5)$$

Hence, the newly proposed model of solar irradiance is reformulated in the dimensionless form and is given by

$$\frac{dy}{ds} = c - y\frac{(y(s-\sigma))^n}{1+(y(s-\sigma))^n} \quad (6)$$

The equilibrium solution, y^* is obtained by solving $c - y^*\frac{(y^*)^n}{1+(y^*)^n} = 0$. Thus, $c - \frac{(y^*)^{n+1}}{1+(y^*)^n} = 0$, or equivalently

$$(y^*)^{n+1} - c(y^*)^n - c = 0 \quad (7)$$

Using substitution of $x = y^*$, we set a function $F(x)$ as

$$F(x) = x^{n+1} - cx^n - c, x \geq 0 \quad (8)$$

which yield

$$F'(x) = (n+1)x^n - cnx^{n-1} = x^{n-1}[(n+1)x - cn], x \geq 0 \quad (9)$$

F is decreases when $F'(x) < 0$ and increases when $F'(x) > 0$. Hence, F decreases for $x < \frac{cn}{n+1}$ and increases for $x > \frac{cn}{n+1}$. In addition, $F(0) = -c < 0$ and $F(\infty) = 0$. Thus, $F(x) = 0$ has a unique positive root $x \in (0, \infty)$. It means that the equilibrium solution $y^* \in (0, \infty)$ is unique and positive. Furthermore,

$$c = \frac{(y^*)^{n+1}}{1+(y^*)^n} < y^* \quad (10)$$

Therefore, Equation (6) has a unique positive equilibrium y^* and that $y^* > c$. Note that, $c = \alpha/\theta\beta$.

We want to prove that Equation (6) has a unique steady state. Suppose K and L are both equilibrium points and $K \neq 0$. We aim to present that $K = L$. The two equilibrium solutions satisfy

$$K^{n+1} - cK^n - c = 0 \quad (11)$$

and,

$$L^{n+1} - cL^n - c = 0 \quad (12)$$

respectively. That means,

$$L^{n+1} - cL^n - c = K^{n+1} - cK^n - c \quad (13)$$

Hence,

$$L^{n+1} - K^{n+1} - c(L^n - K^n) = 0 \quad (14)$$

By applying the formula of

$$a^p - b^p = (a-b)(a^{p-1} + a^{p-2}b + \ldots + ab^{p-2} + b^{p-1}) \quad (15)$$

we obtain

$$(L-K)(L^p + L^{p-1}K + \ldots + LK^{p-1} + K^p$$
$$- c(L^{p-1} + L^{p-2}K + \ldots + LK^{p-2} + K^{p-1})) = 0 \quad (16)$$

Thus, $L - K = 0$ which implies $L = K$. This proves that Equation (6) has a unique equilibrium point. We conduct a linear stability analysis to learn

more about this model's dynamic behaviour. To do this, we apply the Taylor series expansion to linearize the nonlinear system in Equation (6). Consider a system $dy/ds = f(y)$ that has an equilibrium point y^* such that $f(y^*) = 0$. The Taylor series expansion of $f(y)$ around the point y^* is given by

$$f(y) = f(y^*) + \frac{df}{dy}\Big|_{x=y^*}(y - y^*) + \frac{1}{2}\frac{d^2f}{dy^2}\Big|_{x=y^*}(y - y^*)^2 + \frac{1}{6}\frac{d^3f}{dy^3}\Big|_{x=y^*}(y - y^*)^3 + \ldots$$

(17)

and can be simplified as

$$f(y) = f(y^*) + \frac{df}{dy}\Big|_{x=y^*}(y - y^*) + \text{higher order terms}$$

(18)

These higher order terms will be nearly zero when y is sufficiently close to y^*. Hence, we can discard them to attain the approximation as

$$f(y) \approx f(y^*) + \frac{df}{dy}\Big|_{x=y^*}(y - y^*)$$

(19)

Since $f(y^*) = 0$, the approximation near the equilibrium point is given by

$$f(y) = \frac{df}{dy}\Big|_{x=y^*}(y - y^*)$$

(20)

To accomplish the linearization, we specify the perturbation state $Y = y - y^*$. By using the fact that $dY/ds = dy/ds$, we obtain the linearized model given by

$$\frac{dY}{ds} = \frac{df}{dy}\Big|_{y=y^*} Y$$

(21)

Eventually, the resulting linearized equation for

$$dy / ds = c - yF(y(s - \sigma))$$

(22)

is given by

$$\frac{dY(s)}{ds} = -F(y^*)Y(s) - y^*F'(y^*)Y(s - \sigma)$$

(23)

We substitute the exponential solution $Y = Y_0 e^{\mu s}$ which gives

$$\mu + F(y^*) + y^*F'(y^*)e^{-\mu\sigma} = 0$$

(24)

Next, we want to comprehend the behaviour of the roots of the characteristic in Equation (24). If the real part of the characteristic root is negative, then the equilibrium point is stable. Assume that F, F' and y are all positive. If the real part of μ is positive, then

$$\mu + F(y^*) + y^*F'(y^*)e^{-\mu\sigma} > 0$$

(25)

This leads to a contradiction. Therefore, we conclude that the real part of the characteristic root cannot be positive; only the real roots of Equation (24) are negative. Hence, the equilibrium point y^* is stable.

Consequently, we investigate the existence of Hopf bifurcation. Hopf bifurcation occurs when the steady state solution goes unstable with a change of sign of the real part of a complex eigenvalue. Besides that, Hopf bifurcation indicates the presence of oscillatory or periodic solutions in the amount of solar irradiance on the solar panel. Hopf bifurcation can only occur when the parameter values have zero real part and nonzero imaginary part.

In this case, we can set $\mu = i\omega$ indicating that μ has a zero real part. Utilizing the formula of a complex number, $e^{-i\theta} = \cos\theta - i\sin\theta$, we obtain

$$F(y^*) + y^*F'(y^*)\cos\omega\theta + i\omega - iy^*F'(y^*)\sin\omega\sigma = 0$$

(26)

By separating into real and imaginary parts, we obtained two equations. For the real part,

$$F(y^*) + y^*F'(y^*)\cos\omega\theta = 0,$$

(27)

and for the imaginary part,

$$\omega - y^*F'(y^*)\sin\omega\sigma = 0.$$

(28)

We immediately discovered a parametric representation of the critical stability curve from these two expressions given by

$$\omega = y^*F'(y^*)\sin\omega\sigma.$$

(29)

Squaring both sides of equation (29) and employing equation (27), it can be shown that

$$\omega = \sqrt{(y^*F'(y^*))^2 - (F(y^*))^2}.$$

(30)

From equations (27) and (28), it follows that $y^*F'(y^*) = -\frac{F(y^*)}{\cos\omega\theta}$ and $y^*F'(y^*) = \frac{\omega}{\sin\omega\theta}$, respectively. Thus, $\tan\omega\sigma = -\frac{\omega}{F(y^*)}$. The smallest root of this equation lies in the interval $\frac{\pi}{2} < \omega\sigma < \pi$, and the root $\sigma = \frac{1}{\omega}\left[\pi + \tan^{-1}\left(-\frac{\omega}{F(y^*)}\right)\right]$.

Thus, a Hopf bifurcation occurs at the frequency ω and the critical delay σ for a given y^*. The critical stability curve for σ is displayed in Fig. 2. To conclude, if the delay is smaller than this critical delay, then the steady solution is stable. Meanwhile, the steady solution is unstable and exhibits an oscillatory solution if the delay is larger than the critical delay.

4. Results and discussion

The proposed model defined in Equation (2) is solved numerically by employing the 4th-order Runge-Kutta method. The unknown parameters were defined by fitting a parametric curve to the given actual data set by adopting the Nelder-Mead algorithm. The method has been scripted in MATLAB to solve the DDE model. The equation's output defined the predicted amount of solar irradiance reaching the PV module.

The Nelder-Mead algorithm is a numerical optimization method to determine unknown parameters by optimizing an objective function. The algorithm iteratively refines a simplex (a geometric shape) to find the minimum of a function. Simplex is the corner points of a geometric shape. For example, the simplex is a triangle in two dimensions and a tetrahedron in three dimensions. Each vertex of the simplex represents a candidate solution to the optimization problem. These vertices are
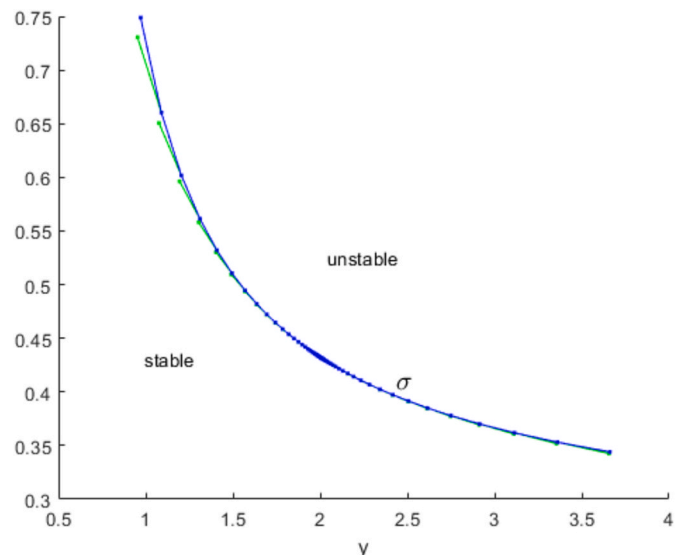

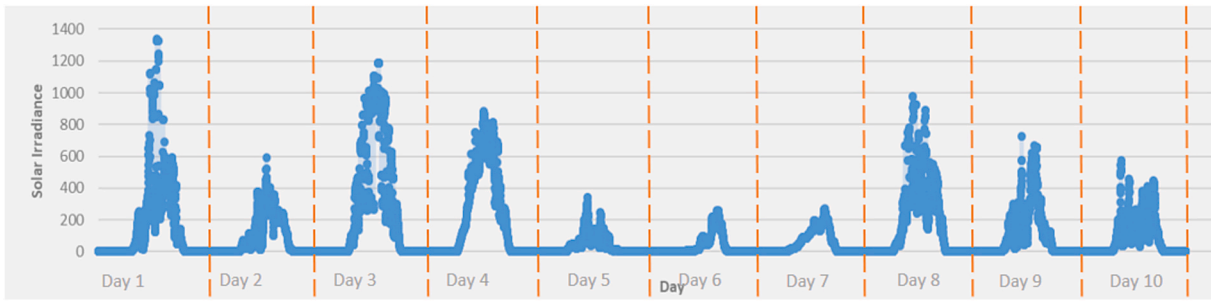**Fig. 2.** Critical stability curve.

Fig. 3. Solar Irradiance from 1st until January 10, 2011.

adjusted and moved around during the algorithm's iteration towards the minimum value of the objective function. The searching process involves some rules of reflection, expansion, contraction, and shrinking on the simplex vertices based on function evaluations. The process continues until convergence is achieved (Nelder and Mead, 1965).

The observation data is collected from a solar PV plant in Pahang Malaysia. The latitude and longitude of the location are $3°32'20.9"N$ and $103°25'47.7"E$ respectively. Data for solar irradiance obtained full cycle is for 2011. Fig. 3 illustrates the ten-day daily pattern of solar irradiance received in a solar PV plant in Pahang, Malaysia, from January 1 to January 10, 2011. During these ten days, the amount of solar irradiance fluctuates and differs for each day. This is due to the dynamic weather profiles at that site location. For example, January 1 was clear day, January 2 was slightly cloud covered and January 6 was heavily overcast. This study considered three types of weather conditions: clear days, slightly cloud-covered, and heavily overcast.

Even though the maximum amount of solar irradiance received is different for each day, the trajectory of solar irradiance resembles a bell-shaped curve similar to that. Because of this reason, Su et al. (2012) utilized a Gaussian curve to model solar irradiance in Macau and discovered that the data was well-fitted.

Typically, one can roughly categorize the changing pattern of solar irradiance within a day into three phases: growth, intermediate, and decay. The growth phase occurs in the morning from 6 a.m. to 9 a.m. when the solar irradiance increases. It is followed by the intermediate phase from 9 a.m. to 4 p.m. when the solar irradiance is relatively high, and the solar irradiance attains its peak at noon, around 12 p.m. Correspondingly, the decay phase happens in the afternoon from 4 p.m. to 7 p.m. when the solar irradiance rapidly declines. Note that, zero solar irradiance was received early in the morning and night.

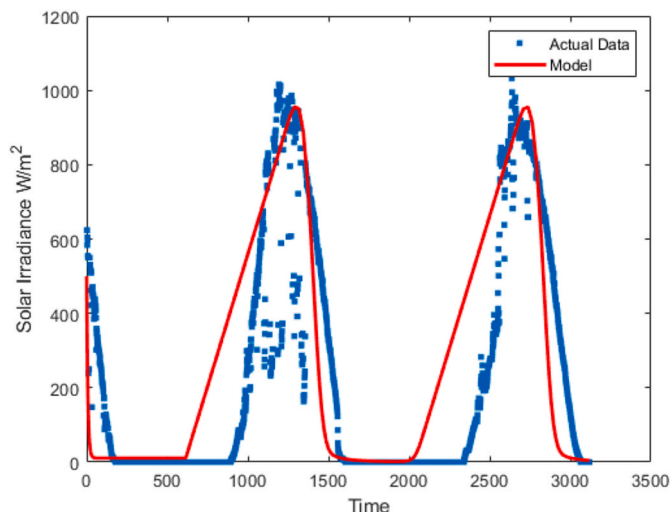This diverse pattern is a consequence of the sun's movement in the

sky each day, which leads to different amounts of solar irradiance obtained at a particular site. The Earth's rotation also causes hourly changes in solar irradiance due to sun's position being low in the sky in the morning and afternoon. Compared to midday, when the sun's position is at its peak, its rays penetrate the atmosphere deeper. Around solar noon on a clear day, a solar collector receives the most solar irradiance.

4.1. Model validation

The profile trajectory of solar irradiance collected on a PV panel during clear days on 2nd – January 4, 2011 is portrayed in Fig. 4. The blue dots denote the actual data, and the red lines represent the model simulation result. By employing the Nelder-Mead algorithm as a parameter fitting technique, the values of the unknown parameters were attained as in Table 2 with the root mean square error (RMSE) value of 2.2735×10^2.

Fig. 5 displays the simulation output for the slightly cloud covered day scenario in accordance with the fitted value of the unknown parameters listed in Table 2. The RMSE value obtained is 2.0292×10^2. The figure illustrated the irregular profile of solar irradiation in cloudy conditions on January 8 to 10, 2011. Typically, on a slightly cloud covered day, the solar irradiance reaches its peak at around 600 W/m2. Additionally, Fig. 6 exhibits the dynamic pattern of solar irradiance during heavily overcast days on January 5 to 7, 2011. The best-fitted parameter values were recorded in Table 2 with the RMSE value 69.7076. The maximum value of solar irradianceattained during heavily overcast days is approximately 250 W/m2.

Based on the results of the three types of weather conditions, as shown in Figs. 4–6, the model is reasonably suitable for the intermediate period (9 a.m. - 4 p.m.) and decay phase (4 p.m.–7 p.m.), but not for the growth phase. Other than that, the model is able to match the peak value of solar irradiance at noon. However, a significant discrepancy exists between the model and the data in the growth phase. It can be seen that the model predicts the growth phase earlier than the actual time. This might be due to the negligence of some factors that affect the solar irradiance dynamic, which should have been included in the formulated model. Note that the incorporation of many factors in a model would increase its complexity which leads to longer running time and requires higher computing performance.

Table 2 display the side-by-side comparison of peak values attained

Fig. 4. Solar irradiance model and actual data for clear-day.

Table 2
Difference between three scenario.

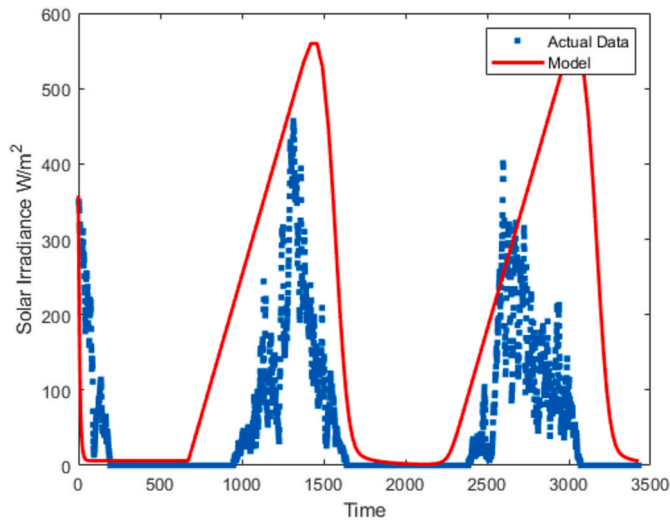| Scenario	Clear Day	Slightly Cloud Covered	Heavily Overcast
Peak Value Constant	1000 W/m^2	600 W/m^2	250 W/m^2
α	1.425	0.75	0.33
β	1581	3704.58	2061.56
θ	10,710	10711.04	12748.07
n	3.06	3.04	1.74
τ	612	669.21	702.95

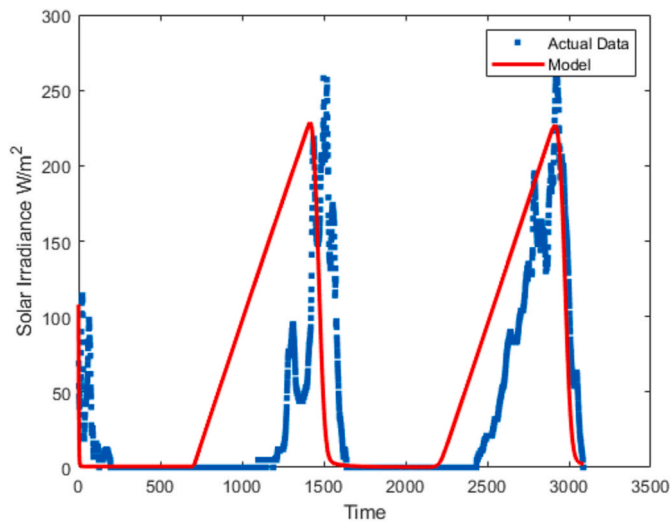**Fig. 5.** Solar irradiance model and actual data for slightly cloud covered day.

Fig. 6. Solar irradiance model and actual data for heavily overcast day.

and the estimated parameters. According to the recorded peak value, the more cloudy the day, the less solar irradiance is received on the solar panel. In addition, the rate of direct and diffused solar irradiance arriving on the solar panel, α is the highest on a clear day and the lowest on a heavily overcast day. In other words, the brighter the day, the greater the value of α.

The time delay, τ on a clear day is the shortest compared to a slightly cloud-covered day and a heavily overcast day. Meanwhile, the longest time delay is discovered on a heavily overcast day. Simply put, the brighter the day, the shorter the time delay for the solar irradiance. On the other hand, solar irradiance transportation from the sun to the solar panel requires a longer time during cloudy days. This is because the cloud cover influenced the diffused solar irradiance as it follows a more scattered and uncertain path through the clouds before reaching the solar panel.

The parameters of β, θ and n are related to the decay rate of solar irradiance. The value of θ and n are almost identical on clear days and days with a slight cloud cover but show a noticeable difference during a heavily overcast. The reason is that the weather conditions of a clear day and a slightly cloud-covered might be close to each other, in contrast to heavily overcast. On the other hand, β did not show any significant pattern from the clear day to slightly cloud-covered and heavily over-

cast. It is a constant that was designed to boost the model's accuracy.

From these findings, we conclude that cloud cover affects the dynamic of solar irradiance. The cloud cover plays a role in reflecting and scattering incoming solar irradiance. An increase in cloud cover would result in a decrease in solar irradiance.

4.2. Time delay simulation

In the proposed model, the time delay value determines the time required for the solar irradiance to reach the solar panel. Thus, the simulation of the time delay can provide valuable insights into the properties of the model. The simulation results during clear days for the parameters listed in Table 3 with different τ are displayed in Figs. 7 and 8.

Note that $\tau = 612$ is the result obtained for clear days. Fig. 7 demonstrates a comparison for the case of $\tau = 400, 612, 800$, where the oscillatory behavior of the solar irradiance is observed. In this case, the systems exhibit a relatively simple behavior, with regular and predictable periodic oscillations. Specifically, as time delay, τ increase, the growth phase of the cycles is delayed but with a higher peak value of solar irradiance.

In contrast, Fig. 8 compares the small value of time delays relative to other parameters i.e. for $\tau = 20, 50, 80, 110$. A small value of the time delay means that solar irradiance has a relatively immediate effect on the solar panel. For $\tau = 20$, the solar irradiance tends to reach its steady state at 200 W/m2. For $\tau = 50, 80$, the graph shows a damped oscillation that converges to a steady state at 200 W/m2.

In this case, the stable steady states at $\tau = 20, 50, 80$ become periodic oscillations at $\tau = 110$. Note that, small changes in the time delay value from $\tau = 80$ to $\tau = 110$ lead to prominent changes in the system's behavior. In other words, the system transitions from a stable steady state to periodic solutions. The effect of incrementing the time delay significantly impacts the solar irradiance behavior. By increasing the delay time, the graph induces oscillations.

When the delay is smaller than the critical delay, the steady solution is stable, which means that small perturbations from the equilibrium state will decay over time, and the system will return to a steady state. Mathematically, this stability is often associated with eigenvalues of the system's linearization having negative real parts, indicating convergence to the equilibrium. In other words, a delay shorter than the critical delay maintains the system's stability. When the delay exceeds the critical delay, the system becomes unstable. This means that small perturbations from the steady state can grow over time, leading to oscillations or divergent behavior. This destabilization is commonly manifested by eigenvalues with positive real parts, indicative of divergence from the equilibrium. The system, in this scenario, tends to exhibit oscillatory behavior.

To summarize, the time delay term in the proposed model significantly affects the dynamic pattern of solar irradiance, where changes in time delay can cause significant changes in the amplitude, peak value and phase of the cycles. In addition, the time delay in the model significantly affects the system's behavior. For example, the time delay value can determine the system's stability and bifurcation properties. In

Table 3

Comparison between three scenario.

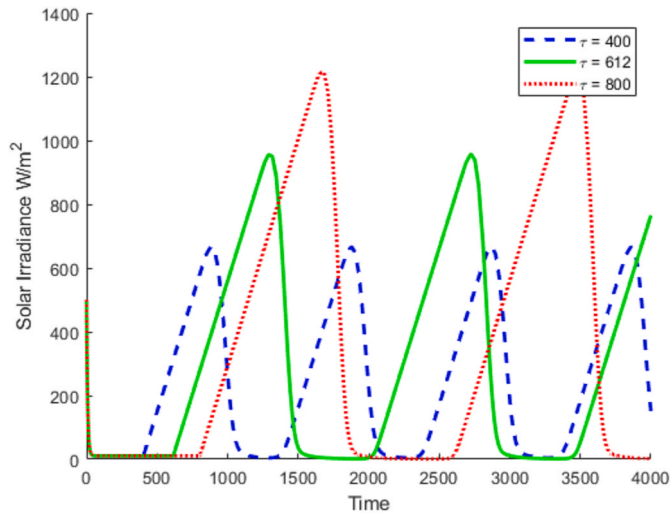| Scenario	Clear Day	Slightly Cloud Covered	Heavily Overcast
Maximum output current, I_0	10.41 A	6.04 A	2.48 A
Maximum output power, P_0	389.36 W	225.76 W	92.61 W
Range of output current in intermediate phase	1.30–10.41 A	0.71–6.04 A	0.55–2.48 A
Range of output power in intermediate phase	48.57–389.36 W	63.80–225.76 W	12.40–92.61 W

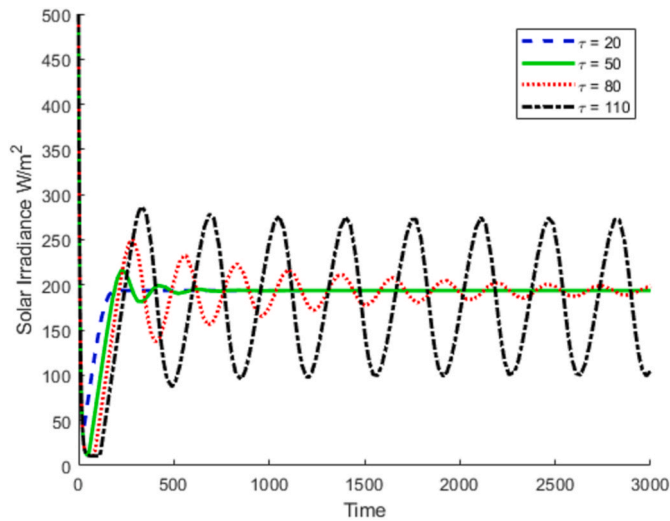**Fig. 7.** Solar irradiance for various values of τ during clear days.

Fig. 8. Solar irradiance for small values of τ during clear days.

addition, it can lead to different types of behavior, such as stability and periodic oscillations.

4.3. The prediction profile of output current and output power

A solar panel produces the output current by absorbing photons from sunlight. Consequently, from the absorption of photons, the PV cells will strike electrons into a higher energy state, generating a flow of electrical current. Correspondingly, the output power of a solar panel is obtained by multiplying the panel's output current and output voltage. The resulting output current is measured in amperes (A), while the output power is measured in watts (W).

The performance of solar PV systems in terms of output current and power is not fixed but changes over time each day. Other than that, the daily changing pattern provides valuable information for designers and users to analyze the performance of their solar PV systems. The objective of this study was to provide a prediction profile for the hourly output current and power depending on the amount of the collected solar irradiance on the panel.

This section focuses on simulating the output current and power for STP250S-20/Wd crystalline solar module. Fig. 9 the trajectory of output current for the three weather conditions: a clear day, a light cloud cover, and a heavy cloud cover. The highest output current is generated on clear days, followed by slightly cloud cover and heavily overcast days. The output current changes significantly depending on the variation in the solar irradiance captured by the PV module. On clear days, a PV module might receive a lot of solar irradiance, whereas, on overcast days, it can receive less. The increase in output current meant more solar irradiance was collected by the PV module, as visualized in Figs. 4–6. Besides the level of solar irradiance, it is important to note that the trajectory of the output current of a solar panel in a day is influenced by other factors. This includes the latitude, the time of year, the weather conditions, the surface area of the panel, the efficiency of the PV cells, the load resistance and the orientation and tilt angle of the panel (Khatib et al., 2012; Mekhilef et al., 2012; Moballegh and Jiang, 2014; Rizal and Wibowo, 2013; Rosario, 2014; Shukla et al., 2015; Zaatri and Azzizi, 2016).

The profile of output current during heavily overcast days is portrayed in Fig. 10. It can be seen that the output current is proportional to the amount of solar irradiance hitting the panel. It is observed that, the peak time for solar irradiance is earlier than that for output power.

In Fig. 11, the output power is compared for three weather conditions: clear day, slightly cloudy, and heavily overcast days. The PV module collects more solar irradiance on clear days, resulting in the highest output power, and less on overcast days. Note that the peak
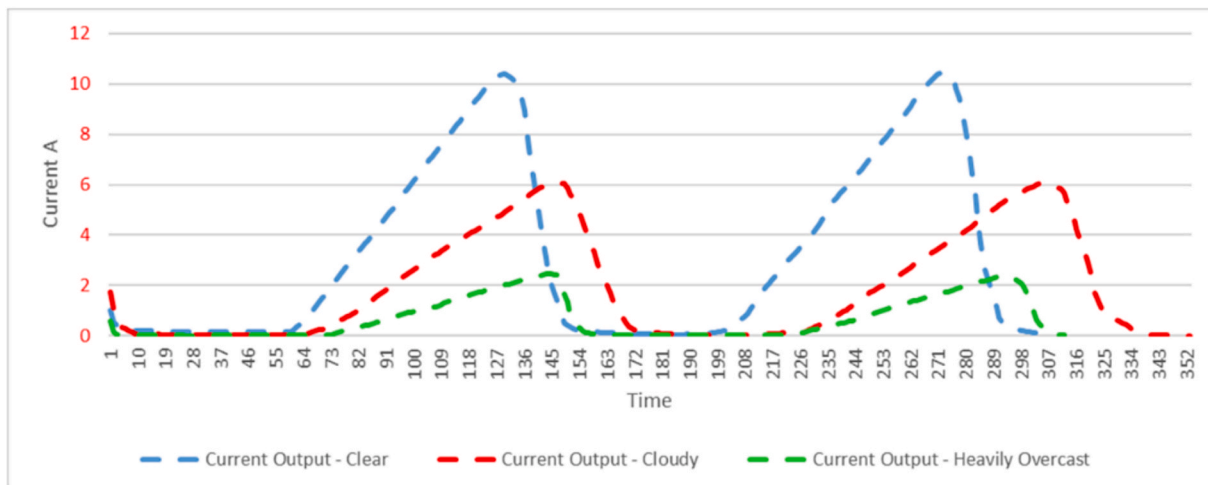

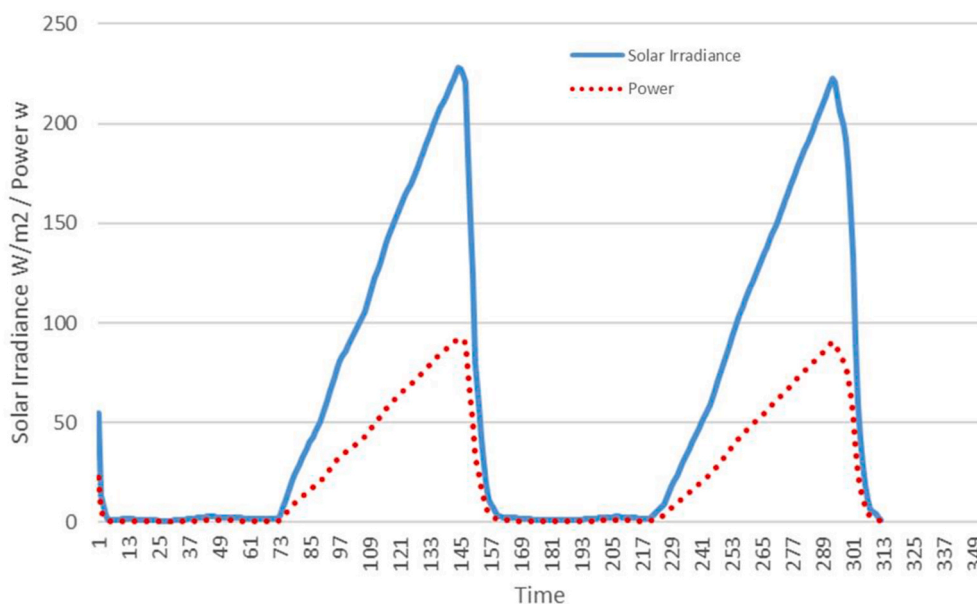**Fig. 9.** Output current for three scenarios.

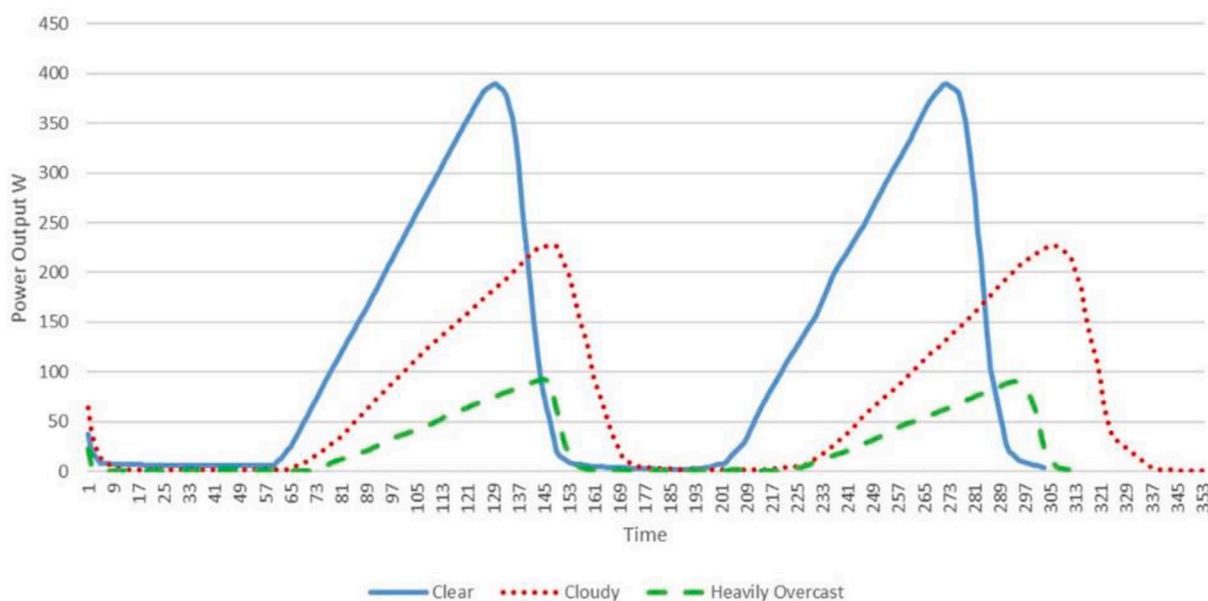**Fig. 10.** Output power and solar irradiance for heavily overcast.

Fig. 11. Output power for three scenarios.

values of solar irradiance and output power are not reached simultaneously. Solar irradiance typically reaches its peak earlier than the output power. Other factors that influence the trajectory of the output current include panel age and condition, PV cell efficiency, panel orientation and tilt angle, shading on the panel, and atmospheric conditions, in addition to solar irradiance level (Khatib et al., 2012; Mekhilef et al., 2012; Moballegh and Jiang, 2014; Rizal and Wibowo, 2013; Rosario, 2014; Shukla et al., 2015; Zaatri and Azzizi, 2016). The prediction profile for hourly output power indicates that it tends to be higher on clear days compared to cloudy days, similar to the trend observed in output current. This is because output power and output current are highly correlated.

Table 3 compares the maximum output current and output power, and the range of output current and output power in intermediate phase of a solar PV module under three different weather conditions: clear,

slightly cloudy, and heavily overcast. According to the results, the maximum output current and power of a PV module decrease by 42% and 76%, respectively, during slightly cloudy and heavily overcast conditions compared to clear days. During the intermediate phase of heavily overcast days, a PV module's output current and power vary slightly, with the smallest range within 0.55–2.48 A and 12.40–92.61 W, respectively. Conversely, a PV module's output current and power value exhibit the largest range during the intermediate phase on clear days within 1.30–10.41 A and 48.57–389.36 W, respectively. Between 9 a.m. and 4 p.m. on slightly cloud covered days, the STP250S-20/Wd crystalline solar module produced output current and power ranging from 0.71 to 6.04 A and 63.80–225.76 W, respectively. Overall, the performance of a PV module is better on clear days compared to cloudy days.

In accordance with the solar irradiance model's result, the consequent performance of solar panels in terms of output current and power

adequately matches the intermediate phase and decay phase. However, it is a bit off for the growth phase. Despite that, it can still provide a valuable purpose for practitioners while focusing on the intermediate and decay phases. Rationally, most PV systems work productively during the intermediate phase from 9 a.m. to 4 p.m. That is the most crucial time to focus on. The depletion of the performance can also be studied through the decay phase.

The key findings of this study were deduced as follows.

i. The changes in solar irradiance will contribute significantly to the output current and the production of output power. As the solar irradiance increases, the output current and power will increase.

ii. The delay time is a crucial factor that must be considered when modelling solar irradiance to reproduce its fluctuations accurately. The delay times would affect the solar irradiance level that arrived on the solar PV panel.

iii. The prediction profile for solar irradiance aligns well with the intermediate and decay phases but deviates slightly during the growth phase. Accordingly, the hourly prediction profiles for output current and power have a similar trend.

iv. The maximum output current and power of STP250S-20/Wd crystalline solar module decrease by 42% and 76%, respectively, during slightly cloudy and heavily overcast conditions when compared to clear days.

v. The amount of energy a solar PV panel produces depends on the weather conditions. The performance of a PV module is better on clear days compared to cloudy days.

vi. This study elucidates the relationship between delayed solar irradiance and the performance of the PV system.

5. Conclusion

Essentially, we made clear connections between the delayed solar irradiance and the performance of a solar PV model. We developed a new mathematical model to predict the solar irradiance that will hit the PV panel and employed the DDE for the first time. Other than that, we succeeded in estimating the unknown parameters related to direct, reflected and diffuse solar irradiance by adopting a parameter fitting technique, the Nelder Mead algorithm. Although many researchers have utilized output current and power as time-independent functions, we treat those equations as time-dependent. The main highlight of the proposed model is that the delay impacts solar irradiance and, consequently, the output current and power produced by the solar PV module. The prediction profile for solar irradiance aligns well with the intermediate and decay phases but deviates slightly during the growth phase. The maximum output current and power of STP250S-20/Wd crystalline solar module decrease by 42% and 76%, respectively, during slightly cloudy and heavily overcast conditions, compared to clear days. The amount of energy a solar PV panel produces depends on the weather conditions. The performance of a PV module is better on clear days compared to cloudy days. The delay factor added value to the solar PV model and increase the understanding of the whole system.

Declaration of competing interest

The authors declare that they have no known competing financial interests or personal relationships that could have appeared to influence the work reported in this paper.

Acknowledgements

Appendix A. Supplementary data

Supplementary data to this article can be found online at https://doi.org/10.1016/j.kjs.2024.100207.

References

Al-Fatlawi, A.W.A., Rahim, N.A., Saidur, R., Ward, T.A., 2015. Improving solar energy prediction in complex topography using artificial neural networks: case study Peninsular Malaysia. Environ. Prog. Sustain. Energy 5 (34), 1528–1535. https://aiche.onlinelibrary.wiley.com/doi/10.1002/ep.12130.

Arief, Y.Z., Aziz, N.A., Pd, A., Aziz, S.S.A., 2017. Evaluation of Solar Energy Potential in Malaysia. https://scialert.net/abstract/?doi=tb.2016.35.43.

Blaha, K., Lehnert, J., Keane, A., Dahms, T., Hövel, P., Schöll, E., Hudson, J.L., 2013. Clustering in delay-coupled smooth and relaxational chemical oscillators. Phys. Rev. 88 (6), 062915 https://doi.org/10.1103/PhysRevE.88.062915.

Campbell, S.A., 2007. Time delays in neural systems. In: Handbook of Brain Connectivity. Springer, Berlin, Heidelberg, pp. 65–90. https://doi.org/10.1007/978-3-540-71512-2_2.

Chen, S.X., Gooi, H.B., Wang, M.Q., 2013. Solar radiation forecast based on fuzzy logic and neural networks. Renew. Energy 60, 195–201. https://doi.org/10.1016/j.renene.2013.05.011.

Chow, C.W., Urquhart, B., Lave, M., Dominguez, A., Kleissl, J., Shields, J., Washom, B., 2011. Intra-hour forecasting with a total sky imager at the UC San Diego solar energy testbed. Sol. Energy 85 (11), 2881–2893. https://doi.org/10.1016/j.solener.2011.08.025.

Danandeh, M.A., 2018. Solar irradiance estimation models and optimum tilt angle approaches: a comparative study. Renew. Sustain. Energy Rev. 92, 319–330. https://doi.org/10.1016/j.rser.2018.05.004.

De Jong, S., Gagliardi, G., Garanto, A., de Breuk, A., Lechanteur, Y.T., Katti, S., et al., 2021. Implications of genetic variation in the complement system in age-related macular degeneration. Prog. Retin. Eye Res., 100952 https://doi.org/10.1016/j.preteyeres.2021.100952.

Hasni, A., Sehli, A., Draoui, B., Bassou, A., Amieur, B., 2012. Estimating global solar radiation using artificial neural network and climate data in the south-western region of Algeria. Energy Proc. 18, 531–537. https://doi.org/10.1016/j.egypro.2012.05.064.

Jamil, N.M., Wang, Q., 2016. CFD-PBE Modelling and simulation of enzymatic hydrolysis of cellulose in a stirred tank. J. Math. Stat. 12 (4), 225–237.

Jiang, Y., 2008. Prediction of monthly mean daily diffuse solar radiation using artificial neural networks and comparison with other empirical models. Energy Pol. 36 (10), 3833–3837. https://doi.org/10.1016/j.enpol.2008.06.030.

Keane, A., Krauskopf, B., Postlethwaite, C.M., 2017. Climate Modelling with Delay Differential Equations.

Khatib, T., Mohamed, A., Mahmoud, M., Sopian, K., 2012. Estimating global solar energy using multilayer perception artificial neural network. Int J Energy 6 (1), 82–87.

Kolesov, Y.S., Shvitra, D.I., 1979. Role of time-delay in mathematical models of ecology. Lithuanian Math. J. 19 (1), 81–91. https://doi.org/10.1007/BF00972005.

Krauskopf, B., 2005. Bifurcation analysis of lasers with delay. Unlocking dynamical diversity: Optical feedback effects on semiconductor lasers 147–183.

Kyrychko, Y.N., Blyuss, K.B., 2005. Global properties of a delayed SIR model with temporary immunity and nonlinear incidence rate. Nonlinear Anal. R. World Appl. 6 (3), 495–507. https://doi.org/10.1016/j.nonrwa.2004.10.001.

Lenstra, D., Yousefi, M., 2000. Theory of delayed optical feedback in lasers. In: AIP Conference Proceedings, vol. 548. American Institute of Physics, pp. 87–111. https://doi.org/10.1063/1.1337760, 1.

Mekhilef, S., Safari, A., Mustaffa, W.E.S., Saidur, R., Omar, R., Younis, M.A.A., 2012. Solar energy in Malaysia: current state and prospects. Renew. Sustain. Energy Rev. 16 (1), 386–396. https://doi.org/10.1016/j.rser.2011.08.003.

Moballegh, S., Jiang, J., 2014. Modelling, prediction, and experimental validations of power peaks of PV arrays under partial shading conditions. IEEE Trans. Sustain. Energy 5 (1), 293–300. https://ieeexplore.ieee.org/document/6676808.

Nelder, J.A., Mead, R., 1965. A simplex method for function minimization. Comput. J. 7 (4), 308–313.

Ozgoren, M., Bilgili, M., Sahin, B., 2012. Estimation of global solar radiation using ANN over Turkey. Expert Syst. Appl. 39 (5), 5043–5051. https://doi.org/10.1016/j.eswa.2011.11.036.

Parmar, K., Blyuss, K.B., Kyrychko, Y.N., Hogan, S.J., 2015. Time-delayed models of gene regulatory networks. Comput. Math. Methods Med. 2015 https://doi.org/10.1155/2015/347273.

Phang, J.C.H., Chan, D.S.H., Phillips, J.R., 1984. Accurate analytical method for the extraction of solar cell model parameters. Electron. Lett. 20 (10), 406. https://doi.org/10.1049/el:19840281.

Pyragas, K., 2006. Delayed feedback control of chaos. Phil. Trans. Math. Phys. Eng. Sci. 364 (1846), 2309–2334. https://doi.org/10.1098/rsta.2006.1827.

Rahman, M., Willmore, B.D., King, A.J., Harper, N.S., 2018. Exponentially-decaying temporal integration in a network model can explain much of the neural sensitivity to stimulus history in primary auditory cortex. bioRxiv, 465047. https://doi.org/10.1101/465047.

Rizal, Y., Wibowo, S.H., 2013. Application of solar position algorithm for sun-tracking system. Energy Proc. 32, 160–165. https://doi.org/10.1016/j.egypro.2013.05.021.

Rosario, A., 2014. Calculating the solar energy of a flat plate collector. Undergraduate Journal of Mathematical Modelling: One+ Two 6 (1), 1. https://doi.org/10.5038/2326-3652.6.1.4857.

Rumbayan, M., Abudureyimu, A., Nagasaka, K., 2012. Mapping of solar energy potential in Indonesia using artificial neural network and geographical information system. Renew. Sustain. Energy Rev. 16 (3), 1437–1449. https://doi.org/10.1016/j.rser.2011.11.024.

Sabudin, S.N., Jamil, N.M., Rosli, N., 2017. A review of parameter estimation used in solar photovoltaic system for a single diode model. J. Phys. Conf. 890 (1), 012037 https://doi.org/10.1088/1742-6596/890/1/012037. IOP Publishing.

Sabudin, S.N.M., Jamil, N.M., 2019. Parameter estimation in mathematical modelling for photovoltaic panel. In: IOP Conference Series: Materials Science and Engineering, vol. 536. IOP Publishing, 012001. https://doi.org/10.1088/1757-899X/536/1/012001, 1.

Sabudin, S.N., Jamil, N.M., Muzakir, S.M., 2020. Mathematical modelling for predicting the performance of photovoltaic module. ASM Sc. J. 13, 2020.

Schöll, E., Hövel, P., Flunkert, V., Dahlem, M.A., 2009. Time-delayed feedback control: from simple models to lasers and neural systems. In: Complex Time-Delay Systems. Springer, Berlin, Heidelberg, pp. 85–150. https://doi.org/10.1007/978-3-642-02329-3_4.

Shampine, L.F., Thompson, S., 2009. Numerical solution of delay differential equations. In: Delay Differential Equations. Springer, Boston, MA, pp. 1–27. https://doi.org/10.1007/978-0-387-85595-0_9.

Shukla, A., Khare, M., Shukla, K.N., 2015. Modelling and simulation of solar PV module on MATLAB/Simulink. International Journal of Innovative Research in Science, Engineering and Technology 4 (1). https://doi.org/10.15680/IJIRSET.2015.0401015.

Su, Y., Chan, L.C., Shu, L., Tsui, K.L., 2012. Real-time prediction models for output power and efficiency of grid-connected solar photovoltaic systems. Appl. Energy 93, 319–326. https://doi.org/10.1016/j.apenergy.2011.12.052.

Widén, J., Munkhammar, J., 2019. Solar Radiation Theory. Uppsala University. https://doi.org/10.33063/diva-381852.

Zaatri, A., Azzizi, N., 2016. Evaluation of some mathematical models of solar radiation received by a ground collector. World Journal of Engineering. https://doi.org/10.1108/WJE-08-2016-050.